No-Reference Image Quality Assessment Using Texture Information Banks

Pedro Garcia Freitas*, Welington Y.L. Akamine† and Mylène C.Q. Farias‡
*Department of Computer Science, †‡Department of Electrical Engineering,
University of Brasília, Brazil
Email: *sawp@sawp.com.br, †welingtonylakamine@gmail.com, ‡mylene@ieee.org

***Abstract*—In this paper, we propose a new no-reference quality assessment method which uses a machine learning technique based on texture analysis. The proposed method compares test images with texture images of a public database. Local Binary Patterns (LBPs) are used as local texture feature descriptors. With a Csiszár-Morimoto divergence measure, the histograms of the LBPs of the test images are compared with the histograms of the LBPs of the database texture images, generating a set of difference measures. These difference measures are used to blindly predict the quality of an image. Experimental results show that the proposed method is fast and has a good quality prediction power, outperforming other no-reference image quality assessment methods.**

***Keywords*—Machine Learning, Computer Vision, Texture Analysis, No-Reference Image Quality Assessment, Texture Information Banks**

I. Introduction

Humans perform many tasks that remain difficult for computers, like for example in pattern recognition tasks. Another example of a task in which humans outperform computers is the quality assessment of a visual content (an image or a video). Quality assessment is becoming increasingly important because of its crucial role in various image processing applications [1], such as compression techniques [2], transmission processes, displays, restoration algorithms [3], or photo enlargement techniques [4, 5].

The most robust method for assessing the quality of images is to use a pool of human observers to evaluate the quality of a given visual content. This process of using humans for assessing the visual quality of images is called subjective quality assessment. In other words, subjective quality assessment methods consist of psychophysical experiments in which human subjects estimate the quality of a series of visual stimuli. Subjective quality assessment methods provide a Mean Opinion Score (MOS) for each visual stimuli, which are the average of the individual scores given by subjects for this stimuli [6]. Psychophysical experiments are expensive, laborious, time-consuming, and, therefore, hard to incorporate into an automatic quality assessment system.

In order to make the process of assessing image quality simpler, many researchers have been developing algorithms that use computers to perform quality assessment tasks. These algorithms are defined as objective image quality assessment (IQA) methods. IQA methods make it possible to implement fast and cheap procedures that can monitor and control the final image quality in several image processing applications. Although a big effort has been dedicated to create efficient algorithms, the development of IQA methods is still a challenging area [1].

Objective image quality assessment methods can be classified in three categories, according to the amount of reference (original) required by the algorithm. Full reference (FR) methods estimate the quality of a test image performing some type of comparison with the reference. Reduced reference (RR) methods use only partial information about the reference image. Since requiring the reference image or even partial reference information is an obstacle for many multimedia applications, the solution is to use no-reference (NR) methods that do not require any information about the reference image.

The development of no-reference image quality assessment (NR-IQA) methods is an even more challenging [7]. Among the the challenges faced by NR-IQA methods, we can cite:

- *Masking models:* The development of accurate masking models are central to determine which image distortions are noticeable and, therefore, which distortions may affect quality.
- *Suprathreshold distortions:* While masking models aim to determine whether distortions are noticeable, they are not suitable for distortions which are beyond the threshold of visibility. For these cases, different perceptual models need to be developed and incorporated into the image quality assessment method.
- *Content effects:* As distortions are superimposed with image content, they can become more or less noticeable depending on the type of visual content. This interaction between the distortion and the content require that IQA methods takes into the consideration the content characteristics.
- *Multiple distortions:* Image processing operations (compression, enhancement, or transmission) can simultaneously insert multiple forms of distortions. Although there are methods for assessing the quality of images subject to a single distortion, the combination of multiple distortions is still an open question.
- *Computational performance:* Although a great effort has been devoted to improve prediction accuracy, state-of-the-art algorithms still present high computational complexity

and, therefore, are not suitable for real-time applications.

To solve the first three challenges listed above, several approaches use distortion-specific (DS) NR-IQA methods, which estimate the strengths of the most relevant distortions in image applications. Among the currently available DS methods, we can cite the works of Wang *et al.* [8], Chabard *et al.* [9], Li *et al.* [10], Farias & Mitra [11], and Manap & Shao [12]. Most of these NR-IQA methods require the knowledge of at least one type of distortion and, therefore, have limited applications in more diverse scenarios.

To add robustness to the incorporation of multiple distortions, non-distortion-specific (NDS) NR-IQA methods must be developed. NDS methods do not require a prior knowledge of the distortions and are, therefore, more adequate for assessing quality in diverse multimedia scenarios. Nevertheless, their design is more challenging. One possible approach consists of using the statistics of natural images [13]–[15]. Another approach that has recently become very popular is the use Machine Learning (ML) techniques. Among the several NR-IQA methods based on machine learning, we can cite the works of Ye *et al.* [16], Zhang *et al.* [17], and Liu *et al.* [18]. Although machine learning techniques show very promising results, they still have limitations in terms of accuracy performance and computational complexity.

In this work, we propose a NDS-NR-IQA method that tackles the aforementioned limitations. The proposed method is a machine learning technique that, unlike other state-of-the-art ML IQA methods, analyses textures to extract information about image content. The algorithm does not make any assumptions about the content or specific distortions. It analyzes the texture information of a test image and compares it with the texture information of a bank of texture images. More specifically, the Csiszár-Morimoto divergence measure is used to compare the histograms of the Local Binary Patterns (LBPs) of the test images with the histograms of the LBPs of the database texture images. These difference measures are used by the ML algorithm to blindly predict the quality of an image.

When compared with state-of-the-art NR-IQA methods, the proposed method has a different approach and shows competitive results. Since it uses simple and fast texture feature extractors based on local binary patterns (LBPs), the proposed method differs from the algorithm proposed by Ye *et al.* [16], which analyzes texture information using large codebooks that store complex Gabor-filter-based features. Although Zhang *et al.* [17] also uses LBPs, their method requires multiple operations with Laplacian of Gaussian (LOG) filters to decompose the images into multi-scale subband images and, then, compute the LBPs for each of these subband images.

This paper introduces the idea of using texture information banks composed by a set of pure textures images. The method uses a dissimilarity representation approach that uses the texture bank as a reference for the test images [19]. Although the proposed approach can be used for feature extraction in other computer vision problems, this study focuses on the development of a robust NDS-NR-IQA method. The proposed approach has the following advantages:

- High accuracy performance;
- Robustness to different distortions;
- Computational efficiency.

The paper is organized as follows. Section II describes the proposed NR-IQA method. Sections III-A and III-B present the experimental setup and results, respectively. Finally, Section IV presents the conclusions.

II. Proposed Method

The proposed method is based on the idea that visual impairments affect image textures. Ideally, the characteristics of features used by a IQA method should change (accordingly) when impairment levels changes, but remain fairly constant when content varies. Unfortunately, visual content affects directly the visibility of impairments and, therefore, their annoyance and the overall image quality. Also, the same content altered with different types of distortions, with nearly the same mean squared error (MSE), can lead to very different values of perceptual quality [20]. To overcome these issues, we represent an image by the statistics of the texture differences. The assumption here is that images with similar distortions and quality levels are represented by similar sets of texture features.

The design of the proposed method is divided into the following stages: (1) construction of a texture information bank, (2) feature vector construction, and (3) image quality prediction using a support vector regression algorithm. In this section, we describe each of these stages.

A. Texture Information Bank

Consider that $\tau = \{T_1, T_2, \cdots, T_n\}$ is a set of n distinct texture images. We want to build a texture information bank, which consists of a set of statistical features extracted from texture images. We use the uniform local binary patterns (LBPs), which is a local operator that has been used to extract fundamental properties of image texture features with a lot of success [21]. The uniform LBP operator is defined as:

$$LBP^{u}_{R,P}(t_c) = \begin{cases} \sum_{p=0}^{P-1} S(t_p - t_c), & U(LBP_{R,P}) \leq 2, \\ P+1, & \text{otherwise}, \end{cases} \quad (1)$$

where

$$U(LBP_{P,R}) = \delta(t_{P-1}, I_0) + \sum_{p=1}^{P-1} \delta(t_p, t_{p-1}), \quad (2)$$

and

$$\delta(t_x, t_y) = |S(t_x - t_c) - S(t_y - t_c)|. \quad (3)$$

In these equations, t_c is the value of the central pixel, t_p is the value of its neighbor, P is the total number of neighbors taken into consideration, R is the radius of this neighborhood, and $S(t)$ is a step function given by:

$$S(t) = \begin{cases} 1 & t \geq 0, \\ 0 & \text{otherwise}. \end{cases} \quad (4)$$

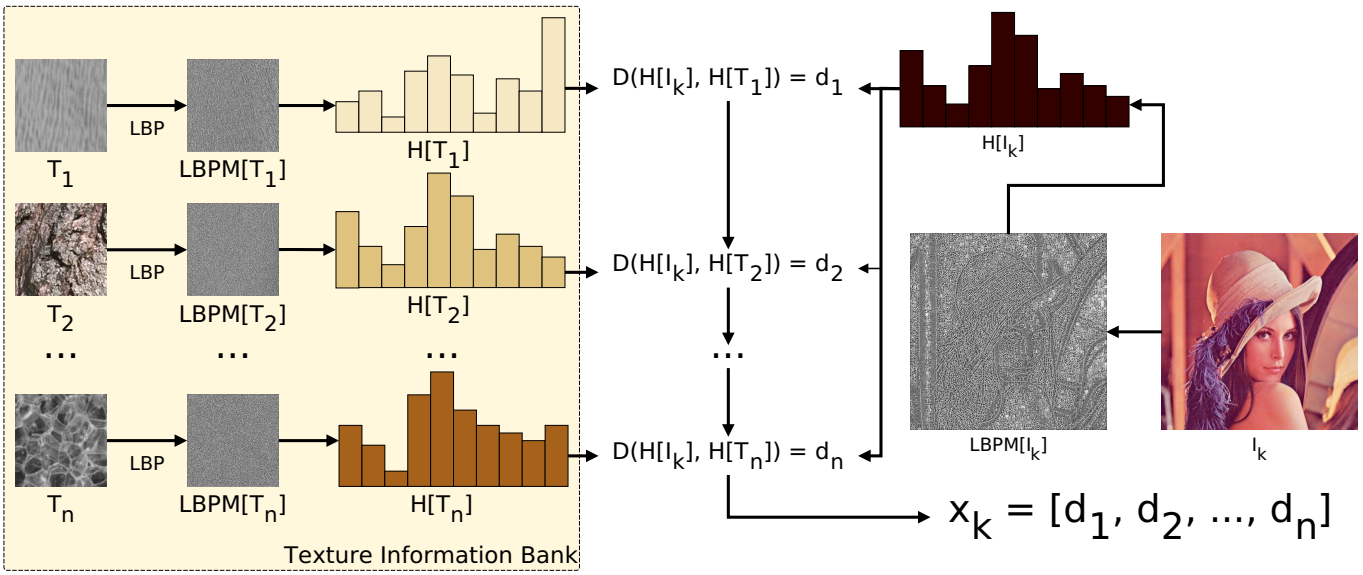

Figure 1: Illustration of the process of extracting the feature vector x_k of a given image I_k. A Csiszár-Morimoto divergence measure (D) is used to compare the LBP-histogram ($H[I_k]$) of I_k and each histogram in the TB.

At the central pixel t_c, each neighboring pixel t_p is assigned with a binary label (0 or 1), depending on their difference. Eq. 1 is computed for each pixel of a given texture image T_j. After the LBPs corresponding to each pixel of T_j are computed, a LBP map of this texture image is built for this set of LBPs. After all LBP maps are computed for all texture images in the set, they are represented as follows:

$$LBPM = \{M_1, M_2, \cdots, M_n\}, \tag{5}$$

where $M_j = \{LBP(T_j(x,y)) : 1 \leq x \leq X, 1 \leq y \leq Y\}$ corresponds to the local binary pattern map of the j-th texture image T_j with dimensions (X, Y). This LBP map is a set that contains the result of processing all pixels of T_j with the LBP operator in Eq. 1.

To extract the statistical information of the j-th texture T_j, we compute the histogram of M_j, as follows:

$$H[T_j] = \{h_j(l_1), h_j(l_2), \cdots h_j(l_{P+1})\}, \tag{6}$$

where

$$h_j(l_i) = \sum_{x,y} f(M_j(x,y), i), \tag{7}$$

and

$$f(v,u) = \begin{cases} 1 & v = u, \\ 0 & v \neq u. \end{cases} \tag{8}$$

In the above equations, (x, y) is the position of a given pixel of M_j and l_i is the i-th LBP label. The histograms computed for each texture $T_j \in \tau$ are stored in the *texture information bank* (TIB): $\eta = \{H[T_1], H[T_2], \cdots, H[T_n]\}$.

B. Feature Vector

Fig. 1 illustrates the process of extracting the feature vector x_k of a given image I_k. This process consists of estimating the distance between the LBP-histogram of the image I_k and each histogram in η. More specifically, given an image I_k, we extract its LBP map and compute its histogram $H[I_k]$, similarly to what was done for textures in the previous section. Then, to obtain the divergences $d_j = D(H[I_k], H[T_j])$ between $H[I_k]$ and each histogram stored in η, we use one of Csiszár-Morimoto divergence measures [22, 23] as D. Since there are n distinct textures, the set $x_k = \{d_1, d_2, \cdots, d_n\}$ is the feature vector associated with image I_k. This feature vector is the input of a support vector regression algorithm to estimate the quality of I_k.

C. Support Vector Regression

After we calculate the feature vector x_k of a given image I_k, we map this information to subjective scores and obtain a quality prediction. We use a support vector regression (SVR) algorithm to predict quality from the feature distance vector. We chose SVR because this machine learning algorithm has been successfully used in other NR-IQA approaches [14, 16]. Also, it is robust for high-dimensional feature spaces [24, 25].

The process of mapping the feature vector x_k to the quality prediction, can be expressed by:

$$Q_p(I_k) = SVR(x_k, \Theta), \tag{9}$$

where Θ is the trained model for regression and $Q_p(I_k)$ is the objective quality score predicted by the model.

III. Experiments

A. Experimental Setup

The experiments were performed by running the simulations on an Intel i7-4790 processor at 3.60GHz. The USC-SIPI Image Database [26] is used to build the TIB. This database contains 64 grayscale texture images, which means that the feature vectors (x_k) for each image have $n = 64$ dimensions. The implementation of SVR uses LibSVM on a Python

Method	JPEG			JPEG2k			WN			GB			FF			ALL		
	SROCC	LCC	KRCC	SROCC	LCC	KRCC	SROCC	LCC	KRCC	SROCC	LCC	KRCC	SROCC	LCC	KRCC	SROCC	LCC	KRCC
PSNR	0.852	0.854	0.644	0.882	0.867	0.694	0.976	0.978	0.893	0.782	0.775	0.586	0.887	0.872	0.700	0.801	0.763	0.596
SSIM	**0.948**	0.809	**0.809**	0.944	0.823	0.806	0.979	0.937	0.882	0.889	0.799	0.733	**0.934**	0.808	0.789	0.890	0.906	0.723
BRISQUE	0.903	0.928	0.744	0.911	0.918	0.750	0.973	0.985	0.882	0.962	**0.967**	0.852	0.883	0.909	0.702	0.934	0.933	0.777
CORNIA	0.924	0.944	0.774	0.933	0.934	0.787	0.967	0.968	0.863	**0.974**	0.969	**0.880**	0.933	**0.928**	**0.793**	0.953	0.944	0.816
CQA	0.887	0.902	0.718	0.897	0.899	0.725	**0.982**	**0.991**	0.906	0.913	0.923	0.754	0.870	0.892	0.704	0.910	0.905	0.740
SSEQ	0.885	0.909	0.704	0.909	0.914	0.740	0.962	0.973	**0.926**	0.936	0.940	0.803	0.853	0.863	0.690	0.901	0.894	0.736
PROPOSED	0.932	**0.955**	0.782	**0.952**	**0.965**	**0.822**	0.974	0.984	0.880	0.963	0.964	0.853	0.891	0.916	0.742	**0.961**	**0.970**	**0.846**

(a) Median SROCC, LCC, and KRCC of simulations on the LIVE2 database.

Method	JPEG		JPEG2k		WN		BLUR		PN		CD		ALL	
	SROCC	LCC	SROCC	LCC	SROCC	LCC	SROCC	LCC	SROCC	LCC	SROCC	LCC	SROCC	LCC
PSNR	0.901	0.894	**0.931**	**0.933**	**0.935**	**0.943**	**0.936**	0.908	**0.932**	**0.955**	**0.886**	**0.899**	0.809	0.786
SSIM	**0.931**	0.875	0.925	0.875	0.876	0.855	0.909	0.810	0.887	0.838	0.813	0.819	0.812	0.722
BRISQUE	0.712	0.804	0.774	0.810	0.642	0.685	0.602	0.732	0.775	0.797	0.508	0.592	0.688	0.761
CORNIA	0.874	0.923	0.903	0.930	0.838	0.857	0.915	**0.948**	0.669	0.671	0.613	0.666	0.787	0.832
CQA	0.632	0.753	0.827	0.870	0.655	0.684	0.618	0.687	0.732	0.761	0.511	0.529	0.653	0.701
SSEQ	0.876	0.904	0.867	0.905	0.916	0.924	0.897	0.929	0.825	0.812	0.703	0.754	0.843	0.858
PROPOSED	0.920	**0.939**	0.864	0.886	0.834	0.852	0.907	0.934	0.825	0.836	0.361	0.393	**0.850**	**0.861**

(b) Median SROCC and LCC of simulations on the CSIQ database.

Method	JPEG			JPEG2k			JPEGXR			ALL		
	SROCC	LCC	KRCC	SROCC	LCC	KRCC	SROCC	LCC	KRCC	SROCC	LCC	KRCC
PSNR	0.793	0.789	0.589	0.863	0.794	0.672	0.804	0.747	0.604	0.814	0.765	0.608
SSIM	0.841	0.887	0.673	0.843	0.850	0.678	0.824	0.843	0.642	0.837	0.865	0.655
BRISQUE	0.881	0.940	0.736	0.869	0.955	**0.810**	0.921	0.950	0.802	0.909	0.931	0.756
CORNIA	0.877	0.932	0.729	0.893	0.924	0.762	0.901	0.948	0.747	0.869	0.917	0.698
CQA	**0.905**	**0.947**	**0.780**	**0.929**	0.939	**0.810**	**0.943**	0.956	**0.824**	**0.921**	0.925	**0.771**
SSEQ	0.800	0.851	0.626	0.904	**0.961**	**0.810**	0.912	0.923	0.780	0.853	0.847	0.687
PROPOSED	0.868	0.921	0.714	0.810	0.845	0.643	0.921	**0.961**	0.790	0.902	**0.946**	**0.771**

(c) Median SROCC, LCC, and KRCC of simulations on the JPEGXR database.

Table I: Correlation indexes across 100 train-test simulations on (a) LIVE2, (b), CSIQ, and (c) JPEGXR databases.

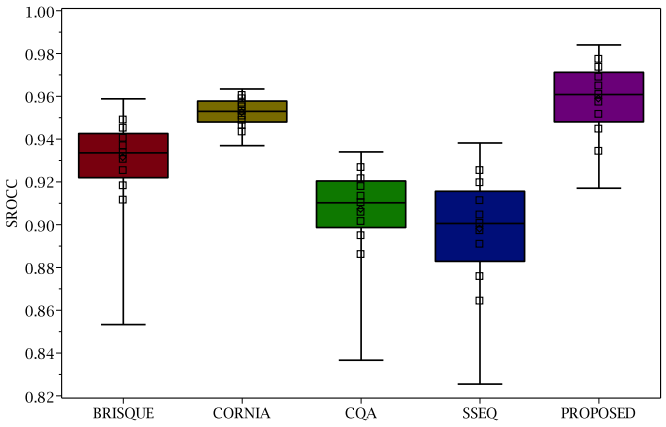

Figure 2: Box plot of SROCC distributions of NR algorithms from 100 runs of simulations using the LIVE2 database.

interface provided by Scikit library. The metaparameters (i.e., kernel, penalty parameter, epsilon, etc.) of the SVR algorithm are found using exhaustive grid search methods provided by the Sklearn's API. The Total Variation [27] is used as the Csiszár-Morimoto divergence D in $d_j = D(H[I_k], H[T_j])$. The parameters of LBP used are: $R = 1$ and $P = 8$.

The proposed algorithm is tested using the following public image quality databases (DB):

- The CSIQ [28] database has a total fo 866 test images, consisting of 30 originals and 6 different categories of distortions.
- The LIVE2 [29] database has 982 test images, including 29 originals and 5 categories of distortions. The distortions include JPEG, JPEG 2000 (JPEG2k), JPEG, white noise (WN), Gaussian blur (GB), fast fading (FF), global contrast decrements (CD), and additive Gaussian pink noise (PN).
- The JPEGXR [30] IQA database has 181 test sequences, including 10 references and 3 type of distortions including JPEG, JPEG 2000, and JPEGXR.

The proposed method is compared with the fastest state-of-the-art NR-IQA methods: BRISQUE [31], CORNIA [16], CQA [32], and SSEQ [33]. In addition to these methods, two well-established FR methods are also tested: PSNR and SSIM [20].

Spearman's Rank Ordered Correlation (SROCC), Pearson (linear) Correlation Coefficient (LCC), and Kendall's Rank Correlation Coefficient (KRCC) are used to evaluate the prediction accuracy of the methods. The correlation coefficients are computed by comparing the subjective scores provided in the databases with the predicted scores obtained using the IQA methods. Since the NR-IQA methods follow a training-based approach, the databases are split into two random subsets, with 80% of data used for training and 20% for testing in each

simulation. Reported results correspond to the median values obtained for 100 random combinations of training and testing subsets.

B. Prediction Performance Evaluation

Tables I (a)-(c) show the correlation coefficients obtained for the considered IQA methods tested on the LIVE2, CSIQ, and JPEGXR databases, respectively. For each database, the tables show SROCC, LCC, and KRCC values obtained for the sets of images containing each distortion type and for the complete set of images (ALL).

For LIVE2 (Table I-a), we can notice that the proposed method surpasses many of the state-of-the-art NR-IQA methods. This can be clearly seen in Fig. 2, which shows the box plot of SROCC distributions for different NR-IQA methods simulations for LIVE2. Notice that the proposed method outperforms the other methods for this database.

For the CSIQ database, the proposed method achieves a statistically better performance than other NR-IQA (see Table I-b). Interestingly, NR approaches perform worse than PSNR for this database. It is worth pointing out that these PSNR scores are consistent with the values reported by Larson and Chandler [28]. Even though the proposed method presents the best overall results, it has the worst performance for CD distortions. We believe the robustness of LBP operators to changes in contrast may be affecting its prediction capability. Further studies are needed to determine whether the performance can be improved with the inclusion of additional features that respond accordingly to contrast.

Results presented in Table I-c indicate that most NR-IQA methods perform statistically close for JPEGXR database. These small differences in performance are probably caused by the fact that test images in JPEGXR database have closer distortions levels than images in the other two databases. This issue can be eliminated by training the algorithm with a larger texture database.

C. Computational Performance Evaluation

Due to the low computational complexity of the LBP operator, the small memory space required by the texture information bank, and the simplicity of the Csiszár-Morimoto divergence, the proposed method has a low data rate and a reduced computational time. As shown in the first line of Table II, the proposed algorithm is considerably faster than other NR-IQA algorithms. The computational advantage of the proposed method is shown more clearly in the second line of Table II, which shows the ratio of the average simulation time of each tested method over the average time of the proposed method. From Table II, we can notice that the proposed method is adequate for real-time applications.

	PSNR	SSIM	BRISQUE	CORNIA	CQA	SSEQ	PROPOSED
Time	0.0055	0.0447	0.1576	1.8964	1.3691	1.8112	0.0323
Speedup	0.1702	1.3839	4.8792	58.7121	42.3869	56.0743	1.0000

Table II: Average computational time for performing an objective quality assessment (in seconds).

D. Discussion

1) Implementation Complexity: Although the proposed method has shown great advantage in terms of execution time compared to other methods, there are some considerations about the speed that are worth discussing. First, the implementation of the proposed algorithm uses a non-optimized Python implementation. Therefore, we must point out that the algorithm can be further optimized in order to become more attractive for real-time multimedia applications. Second, all operations used to compute the LBP maps are performed independently for each pixel. Likewise, the Csiszár-Morimoto divergence measures are also computed independently for each texture. Hence, the performance of the proposed method can be improved with a parallel implementation of the algorithm. Moreover, due to simplicity of the LBP operator, which uses only relational operators and sums, it is also possible to implement the proposed method in a dedicated hardware.

2) Modularity: The texture information bank approach has the advantage of representing the image in terms of textures. It does not depend on the knowledge of specific distortions. Therefore, the proposed method is modular and can be expanded to any number of distortions. New distortions can be inserted in the model by adding images with these distortions in the training set.

3) Applicability: Despite the fact that the texture information bank has been presented as a strategy to extract features for predicting visual quality of images, the proposed method could be adapted for other applications. Particularly, computer vision applications based on texture analysis are possible candidates to use this technique. Among possible applications, we can cite texture classification [34], face spoofing detection [35, 36], gender recognition [37], expression recognition [38], etc.

IV. Conclusions

This paper presents a new NR-IQA method that requires no previous assumption about the type of distortions in the test images. The method uses a machine learning technique based on a very efficient texture analysis strategy, what makes it faster and simpler than other NR-IQA methods. Results show that the proposed method has a competitive quality prediction performance, when compared with state-of-the-art NR-IQA methods. Future works include the investigation of the impact of the method parameters (including the size of the texture information bank and the statistical properties of textures) on accuracy of the predicted quality. Furthermore, it is important to investigate if the addition of contrast and color features can improve the prediction performance for images affected with these types of distortions.

References

[1] Z. Wang, A. C. Bovik, and L. Lu, "Why is image quality assessment so difficult?" in *Acoustics, Speech, and Signal Processing (ICASSP), 2002 IEEE International Conference on*, vol. 4. IEEE, 2002, pp. IV–3313.

[2] S. Wang, A. Rehman, Z. Wang, S. Ma, and W. Gao, "Ssim-inspired divisive normalization for perceptual video coding," in *Image Processing (ICIP), 2011 18th IEEE International Conference on*. IEEE, 2011, pp. 1657–1660.

[3] X. Liu, D. Zhai, D. Zhao, G. Zhai, and W. Gao, "Progressive image denoising through hybrid graph laplacian regularization: a unified framework," *Image Processing, IEEE Transactions on*, vol. 23, no. 4, pp. 1491–1503, 2014.

[4] X. Liu, D. Zhao, J. Zhou, W. Gao, and H. Sun, "Image interpolation via graph-based bayesian label propagation," *Image Processing, IEEE Transactions on*, vol. 23, no. 3, pp. 1084–1096, 2014.

[5] C. Mori, M. Sugie, H. Takeshita, and S. Gohshi, "Subjective assessment of super-resolution," in *Information and Telecommunication Technologies (APSITT), 2015 10th Asia-Pacific Symposium on*. IEEE, 2015, pp. 1–3.

[6] M. H. Pinson, L. Janowski, and Z. Papir, "Video quality assessment: Subjective testing of entertainment scenes," *IEEE Signal Processing Magazine*, vol. 32, no. 1, pp. 101–114, 2015.

[7] D. M. Chandler, "Seven challenges in image quality assessment: past, present, and future research," *ISRN Signal Processing*, vol. 2013, 2013.

[8] S. Wang, C. Deng, B. Zhao, G.-B. Huang, and B. Wang, "Gradient-based no-reference image blur assessment using extreme learning machine," *Neurocomputing*, vol. 174, pp. 310–321, 2016.

[9] T. Chabardès and B. Marcotegui, "Local blur estimation based on toggle mapping," in *Mathematical Morphology and Its Applications to Signal and Image Processing*. Springer, 2015, pp. 146–156.

[10] L. Li, Y. Zhou, W. Lin, J. Wu, X. Zhang, and B. Chen, "No-reference quality assessment of deblocked images," *Neurocomputing*, vol. 177, pp. 572 – 584, 2016.

[11] M. Farias and S. Mitra, "No-reference video quality metric based on artifact measurements," in *Image Processing, 2005. ICIP 2005. IEEE International Conference on*, vol. 3, Sept 2005, pp. III–141–4.

[12] R. A. Manap and L. Shao, "Non-distortion-specific no-reference image quality assessment: A survey," *Information Sciences*, vol. 301, pp. 141–160, 2015.

[13] M. A. Saad, A. C. Bovik, and C. Charrier, "Blind image quality assessment: A natural scene statistics approach in the dct domain," *Image Processing, IEEE Transactions on*, vol. 21, no. 8, pp. 3339–3352, 2012.

[14] A. K. Moorthy and A. C. Bovik, "Blind image quality assessment: From natural scene statistics to perceptual quality," *Image Processing, IEEE Transactions on*, vol. 20, no. 12, pp. 3350–3364, 2011.

[15] Y. Fang, K. Ma, Z. Wang, W. Lin, Z. Fang, and G. Zhai, "No-reference quality assessment of contrast-distorted images based on natural scene statistics," *Signal Processing Letters, IEEE*, vol. 22, no. 7, pp. 838–842, 2015.

[16] P. Ye, J. Kumar, L. Kang, and D. Doermann, "Unsupervised feature learning framework for no-reference image quality assessment," in *Computer Vision and Pattern Recognition (CVPR), 2012 IEEE Conference on*. IEEE, 2012, pp. 1098–1105.

[17] M. Zhang, C. Muramatsu, X. Zhou, T. Hara, and H. Fujita, "Blind image quality assessment using the joint statistics of generalized local binary pattern," *Signal Processing Letters, IEEE*, vol. 22, no. 2, pp. 207–210, 2015.

[18] L. Liu, Y. Hua, Q. Zhao, H. Huang, and A. C. Bovik, "Blind image quality assessment by relative gradient statistics and adaboosting neural network," *Signal Processing: Image Communication*, vol. 40, pp. 1–15, 2016.

[19] R. P. Duin, E. Pekalska, P. Paclik, and D. M. Tax, "The dissimilarity representation, a basis for domain based pattern recognition," in *Pattern representation and the future of pattern recognition, ICPR 2004 Workshop Proceedings, Cambridge, UK*, 2004, pp. 43–56.

[20] Z. Wang, A. C. Bovik, H. R. Sheikh, and E. P. Simoncelli, "Image quality assessment: from error visibility to structural similarity," *Image Processing, IEEE Transactions on*, vol. 13, no. 4, pp. 600–612, 2004.

[21] T. Ojala, M. Pietikäinen, and T. Mäenpää, "Multiresolution gray-scale and rotation invariant texture classification with local binary patterns," *Pattern Analysis and Machine Intelligence, IEEE Transactions on*, vol. 24, no. 7, pp. 971–987, 2002.

[22] T. Morimoto, "Markov processes and the h-theorem," *Journal of the Physical Society of Japan*, vol. 18, no. 3, pp. 328–331, 1963.

[23] A. Cichocki and S.-i. Amari, "Families of alpha-beta-and gamma-divergences: Flexible and robust measures of similarities," *Entropy*, vol. 12, no. 6, pp. 1532–1568, 2010.

[24] A. J. Smola and B. Schölkopf, "A tutorial on support vector regression," *Statistics and computing*, vol. 14, no. 3, pp. 199–222, 2004.

[25] M. Minghui and Z. Chuanfeng, "Application of support vector machines to a small-sample prediction," *Advances in Petroleum Exploration and Development*, vol. 10, no. 2, pp. 72–75, 2016.

[26] A. G. Weber, "The USC-SIPI image database version 5," *USC-SIPI Report*, vol. 315, pp. 1–24, 1997.

[27] I. Sason and S. Verdú, "Upper bounds on the relative entropy and rényi divergence as a function of total variation distance for finite alphabets," in *Proceedings of the 2015 IEEE Information Theory Workshop (ITW 2015)*, 2015, pp. 214–218.

[28] E. C. Larson and D. M. Chandler, "Most apparent distortion: full-reference image quality assessment and the role of strategy," *Journal of Electronic Imaging*, vol. 19, no. 1, p. 011006, 2010. [Online]. Available: http://link.aip.org/link/?JEI/19/011006/1

[29] H. R. Sheikh, M. F. Sabir, and A. C. Bovik, "A statistical evaluation of recent full reference image quality assessment algorithms," *Image Processing, IEEE Transactions on*, vol. 15, no. 11, pp. 3440–3451, 2006.

[30] F. De Simone, L. Goldmann, V. Baroncini, and T. Ebrahimi, "Subjective evaluation of jpeg xr image compression," in *SPIE Optical Engineering+ Applications*. International Society for Optics and Photonics, 2009, pp. 74 430L–74 430L.

[31] A. Mittal, A. K. Moorthy, and A. C. Bovik, "No-reference image quality assessment in the spatial domain," *Image Processing, IEEE Transactions on*, vol. 21, no. 12, pp. 4695–4708, 2012.

[32] L. Liu, H. Dong, H. Huang, and A. C. Bovik, "No-reference image quality assessment in curvelet domain," *Signal Processing: Image Communication*, vol. 29, no. 4, pp. 494–505, 2014.

[33] L. Liu, B. Liu, H. Huang, and A. C. Bovik, "No-reference image quality assessment based on spatial and spectral entropies," *Signal Processing: Image Communication*, vol. 29, no. 8, pp. 856–863, 2014.

[34] J. Xie, L. Zhang, J. You, and S. Shiu, "Effective texture classification by texton encoding induced statistical features," *Pattern Recognition*, vol. 48, no. 2, pp. 447–457, 2015.

[35] Z. Boulkenafet, J. Komulainen, and A. Hadid, "face anti-spoofing based on color texture analysis," in *Image Processing (ICIP), 2015 IEEE International Conference on*. IEEE, 2015, pp. 2636–2640.

[36] A. Benlamoudi, D. Samai, A. Ouafi, A. Taleb-Ahmed, S. E. Bekhouche, and A. Hadid, "Face spoofing detection from single images using active shape models with stasm and lbp," in *Proceeding of the Troisime Conference Internationale Sur La Vision Artificielle CVA 2015*, 2015.

[37] A. Hadid, J. Ylioinas, M. Bengherabi, M. Ghahramani, and A. Taleb-Ahmed, "Gender and texture classification: A comparative analysis using 13 variants of local binary patterns," *Pattern Recognition Letters*, vol. 68, pp. 231–238, 2015.

[38] A. Ramirez Rivera, J. Rojas Castillo, and O. Chae, "Local directional number pattern for face analysis: Face and expression recognition," *Image Processing, IEEE Transactions on*, vol. 22, no. 5, pp. 1740–1752, 2013.